

Supplementary Information for:
Activation of Rho-family small GTPases by small molecules

Charuta C. Palsuledesai^{3,4#}, Zurab Surviladze^{1,3#‡}, Anna Waller^{1,3}, T. Fabiola Miscioscia^{2,6#‡}, Yuna Guo^{3,4‡}, Yang Wu^{1‡}, Jake Strouse^{1‡}, Elsa Romero^{3,4}, Virginia M. Salas^{1‡}, Ramona Curpan^{2,5}, Susan Young^{1‡}, Mark Carter^{1‡}, Terry Foutz^{1‡}, Zhanna Galochkina³, Harold Ames¹, Mark K. Haynes^{1,3}, Bruce S. Edwards^{1,3,4‡}, Orazio Nicolotti⁶, Li Luo^{3,7}, Oleg Ursu², Cristian G. Bologa², Tudor I. Oprea^{2,3}, Angela Wandinger-Ness^{3,4\$,*} and Larry A. Sklar^{1,3,4, §}

¹Center for Molecular Discovery; ²Translational Informatics Division, Department of Internal Medicine; ³Comprehensive Cancer Center; ⁴Department of Pathology, University of New Mexico School of Medicine, Albuquerque, NM 87131, ⁵Institute of Chemistry, Romanian Academy, Timisoara, Romania. ⁶Dipartimento di Farmacia-Scienze del Farmaco, Università di Bari 'Aldo Moro', Via Orabona, 4, 70126, Bari, Italy; ⁷Division of Epidemiology, Department of Internal Medicine, University of New Mexico School of Medicine, Albuquerque, NM 87131.

#Authors contributed equally to the work; §Senior authors contributed equally.

*Correspondence should be addressed to:

Dr. Angela Wandinger-Ness
Dept. Pathology MSC 08 4640
University of New Mexico HSC
Albuquerque, New Mexico 87131
Phone: 505-272-1459
FAX: 505-272-4193

Supplementary Methods

Reagents and Cell Lines

BODIPY® (4,4-difluoro-4-bora-3a,4a-diaza-s-indacene or dipyrromethene-boron-difluoride) nucleotide analogues (BODIPY FL GTP 2'-(or-3')-O-(N-(2-aminoethyl) urethane, G-12411 from Invitrogen Molecular Probes.¹ GST-GTPase chimeras were purchased from Cytoskeleton Inc. or purified from *E. coli* (Rab2, Rab7) as described.² Bead sets for multiplex assays were provided by Duke Scientific Corp. (Fremont, CA) following protocols developed by the NMMLSC.³ A mouse pan-Rac mAb (recognizes Rac1-3) was from BD Biosciences (#610650, San Jose, CA) and a mouse mAb specific for Rac1 and rhodamine phalloidin were from Cytoskeleton, Inc (#ARC03). ECL reagent kit was purchased from Pierce (ThermoFisher Scientific), Rockford, IL. GST-PAK-PBD attached to glutathione beads was a generous gift from Dr. G. Bokoch (The Scripps Research Institute). GLISA kit to measure Cdc42 activity, and His-DBS (DH/PH domain) were purchased from Cytoskeleton, Inc. (Denver, CO). Compounds for the primary screen were from the Molecular Libraries Screening Center Network. For dose response assays, compounds predicted by virtual screening were purchased from ChemDiv Inc. (San Diego, CA), ChemBridge™ (San Diego, CA) or Ryan Scientific, Inc. (Mt. Pleasant, SC). Compound identification numbers (CID) are given for all test compounds used and may be used to track individual compounds in PubChem. Esterified variants were synthesized by Alexander Kornienko (New Mexico Institute of Mining and Technology, Socorro, NM). All other reagents were from Sigma-Aldrich (St. Louis, MO) unless otherwise specified.

RBL-2H3 and Swiss 3T3 cells 55 were cultured as described.^{4, 5} Compounds were administered to cells in DMSO (1% final) and vehicle controls were treated with 1% DMSO alone.

Mass Spectrometry

Purchased lead compounds were confirmed by high resolution mass spectrometry (HRMS). HRMS (m/z): CID888706 from ChemBridge™ (San Diego, CA) [M]⁻ calculated for C₁₄H₁₃NO₂S, 258.0589; experimental, 258.0585; CID7345532 from ChemDiv Inc. (San Diego, CA) [M]⁻ calculated for C₁₉H₁₉NO₃, 308.1287; experimental, 308.1292; CID2160985 from Ryan Scientific, Inc. (Mt. Pleasant, SC) [M]⁻ calculated for C₁₄H₁₁BrO₃, 304.9813 (for the ⁷⁹Br isotope); experimental, 304.9819.

Multiplexed Primary Screens and Statistical Analyses

Bead sets were coated with individual GST-GTPase chimeras as described.⁶ Briefly, glutathione beads in each set were similar in size (~4 μm diameter), yet distinguishable seven different intensities of red color (various magnitude of emission at 665 \pm 10 nm with excitation at 635 nm). Using GST-GFP, $\sim 10^6$ glutathione sites per bead were estimated. 240-250 μL of each bead set was blocked with 0.1% BSA in NP-HPSE buffer (0.01% NP-40, 30 mM HEPES pH 7.5, 100 mM KCl, 20 mM NaCl and 1 mM EDTA) at RT for 30 min. Beads from each set were resuspended in 100 μL of NP-HPSE and individually incubated overnight with 1 μM of GST-tagged GTPases (Cdc42, Rab2, Rab7, activated Rac1Q61L, Rac1 and H-Ras) at 4 $^{\circ}\text{C}$. Beads were then washed twice with cold NP-HPSE containing 0.1% BSA and 1 mM DTT. Bead sets coated with different GTPase chimeras were pooled together, and this mixture was used for multiplex analyses of GTP binding. The assay was conducted in 384-well microplates in a total well volume of 10.1 μL (5 μL protein-coated beads in NP-HPSE, 0.1 μL of test compound, and 5 μL 200 nM BODIPY-FL-GTP (in NP-HPSE for a final concentration of GTP of 100 nM)). Positive controls, containing bead mixtures and fluorescent GTP but no test compound, were located in columns 1 and 2 on each plate. Negative controls, containing bead mixtures with fluorescent GTP and 0.5 μM unlabeled GTP, were assayed separately. Plates were placed on rotators and incubated for 40–45 min at 4 $^{\circ}\text{C}$. Sample analysis was conducted with the HyperCyt[®] high throughput flow cytometry platform as described previously.^{3, 7} HyperCyt consists of an autosampler connected to a peristaltic pump: the autosampler sips ~2 μL of suspension from each of the wells of a multi-well plate, leaving an air gap between samples. Flow cytometric light scatter and fluorescence emission at 530 \pm 20 nm (FL1) and 665 \pm 10 nm (FL8) were collected on a Cyan ADP flow cytometer (Beckman Coulter, Fullerton, CA). The resulting time-dependent data (1 file/plate) was analyzed using IDLeQuery software (available free from the authors) to determine the compound activity in each well. Gating based on FL8 emission distinguishes the beads coated with different proteins, and the median fluorescence per bead population was calculated. Compounds that satisfied hit selection criteria in the primary screen (change in % activity higher than 20% from baseline) were cherry-picked from compound storage plates and tested to confirm activity and determine potency. A total of 194,635 compounds were screened of which 1877 were identified as hits. A total of 1281 unique compounds were tested in secondary screens yielding 198 unique active compounds with 77 inhibitors and 43 activators. The complete results of the primary screens and secondary dose responses for all GTPases tested are posted on PubChem under (AID

757-761, 764; 1334-1336, 1339-1341). For primary screens, average Z' values (established coefficient for assay quality based on dynamic range and data variation⁸) were calculated for each target using IDLeQuery to extract and pool gated data from positive and negative control wells. For secondary dose response measurements, ligand competition curves were fitted by Prism (GraphPad Software, Inc., San Diego, CA) using nonlinear least-squares regression in a sigmoidal dose response model with variable slope, also known as the four parameter logistic equation.

Virtual Screening and Structural Analysis

The ROCS program was used for virtual screening of the ChemDiv discovery library collection of over 700,000 compounds.^{9, 10} ROCS uses shape (3D) similarity to select small molecules that resemble the query. Three compounds (CID: 888706, 7345532, 2160985) were selected based on the COMBO score (shape similarity and Color Force Field), which ranks molecules based on both shape and chemical similarity. To calibrate the ROCS settings, the three selected query molecules were used to screen 14,500 compounds from MLSMR that have a carboxylic acid group in section A of the general structure. For each query, 500 compounds were selected by default with a COMBO score above a 1.5 cutoff. Thirty-three out of 1087 MLSMR hits were ranked in the top 4% of the complete list, confirming the reliability of the search method. Subsequently, the three queries were used to virtually screen the ChemDiv database using the calibrated ROCS settings; selected molecules were experimentally tested in the multiplex GTP-binding assay. Subsequently, all the compounds selected from MLSMR and ChemDiv libraries were analyzed through cluster analysis and SAR studies to identify the structural elements that were important for biological activity.

Dose Response Measurements and Selection Criteria for Active Compounds

Test compounds identified for further analysis were serially diluted 1:3 eight times from a starting concentration of 10 mM for a total of 9-point dilution series in DMSO. The final concentrations in the assay ranged from 10 nM-100 μ M. In total 1236 compounds were tested in dose response assays based on both MLSMR and ChemDiv virtual screening.

Changes in GTP binding affinity (Kd) and Bmax in the presence of a given compound were measured in multiplex (Cdc42, Cdc42Q61L, Rab2, Rab7, H-Ras and H-RasG12V) and single-plex formats (Rac1, Rac1Q61L and GST-GFP). GTPases and the GST-GFP control were individually bound to glutathione beads overnight at 4°C, washed with HPSE buffer, then

resuspended together or assayed individually in the same buffer containing DTT and BSA. Bound GTPases were analyzed by mixing 5 μ l protein-bound beads with 2.5-100 nM BODIPY-GTP in a total volume of 10 μ l and incubating with rotation at 4°C for 90 min. DMSO controls and samples treated with 10 μ M of each test compound were run in parallel. Bound fluorescent nucleotide was measured using a Cyan ADP flow cytometer. Data were converted to ASCII format using IDLeQuery, exported and analyzed using Prism (GraphPad Software, Inc., San Diego, CA) non-linear, one-site binding. Bound fluorescent nucleotide was measured using a Cyan ADP flow cytometer with Summit V4.3.03 Build 2456 from Beckman Coulter, Inc (Brea, CA). Data were binned for separating and annotating assay plate wells by using HyperView (in-house developed software by Bruce Edwards). Exported data was further analyzed using Prism (GraphPad Software, Inc., San Diego, CA) non-linear, one-site binding.

GTPase activators were identified on the basis of an increase in fluorescent GTP-binding. In dose response assays, the following seven criteria were used to identify active compounds: (1) $-8 < \text{LOGEC}_{50} < -4$ (the computed EC₅₀ value should be in the interval of tested concentrations); (2) $0.5 < |\text{HILLSLOPE}| < 2$ (the absolute value of HILLSLOPE should be higher than 0.5 and lower than 2); (3) $[\text{TOP} - \text{STD_TOP}] > [\text{BOTTOM} + \text{STD_BOTTOM}]$ (the amplitude of the biological signal should be statistically significant); (4) $|\text{LOGEC}_{50}| > \text{STD_LOGEC}_{50}$ (the standard error of LOGEC₅₀ should be lower than the absolute value of LOGEC₅₀); (5) $|\text{HILLSLOPE}| > \text{STD_HILLSLOPE}$ (idem for the HILLSLOPE); (6) $[\text{TOP} - \text{BOTTOM}] \text{ scavenger} < 0.1 * [\text{TOP} - \text{BOTTOM}] \text{ target}$ (the inherent fluorescence of the test compound should be lower than 10% of the biological signal); (7) $[\text{TOP} - \text{BOTTOM}] / \text{TOP for GST-GFP} < 0.1 * [\text{TOP} - \text{BOTTOM}] / \text{TOP for the target}$ (the interference of the compound with the GST/GSH interaction should be lower than 10% of the biological signal). NB: We previously demonstrated that high site density binding on glutathione beads lowers dissociation of GST-tagged proteins.¹¹ The experiments performed in this manuscript were carried out under the saturating levels of GST-GTPase chimeras bound to glutathione beads, to prevent dissociation of bound GTPases. In the event a small amount of GST-GTPase dissociates off the beads, it was desirable to limit its association to a different set of beads considering the multiplex experimental set up. Therefore, scavenger beads were used to capture any such dissociated proteins to limit scrambling of beads (multiple types of GST-GTPases on a single bead). The strategy allows quantification of the levels of free GTPases in solution during the assay, which was found to be low based on the measured B_{max} values for the scavenger beads.

SAR for Three Chemical Families of GTPase Activators

SAR analysis was conducted in order to identify the structure determinants important for biological activity. Because all compounds behaved as pan GTPase activators in all SAR series the following discussions are focused on activity across all tested targets for each compound series. Although the exact activator binding site on the GTPases is not definitively known, kinetic and cell-based assays suggest the compounds in all three series bind to an allosteric site and have the same mode of action. Shape overlays of lead compounds from all three series, demonstrates good overlap between these structures which further suggests that these compounds can bind in similar modes to the GTPase targets (Figure S6).

Nicotinic Acid Series. The following structural features were required for biological activity in this series of compounds. Section A is usually an unsubstituted nicotinic acid moiety, any substitution in this section leads to total or significant loss of biological activity. Section B of the compound is usually a benzene ring substituted with small, preferably non-polar substituents like methyl, methoxy, halogen, polar substituents. Larger polar substituents like nitro or aldehyde groups rendered the compound inactive. The linker region connecting moieties A and B is usually between 1-4 atoms long. The first linker atom attached to the nicotinic acid must be sulfur, oxygen, or nitrogen and the most potent compounds have a sulfur heteroatom in the linker. The best compound in the series CID888706 has an unsubstituted nicotinic acid moiety linked with 3 atom linker to the unsubstituted benzene ring in section B. A total of 26 compounds from this series were tested in dose response assays of which 16 were found to be active (Supplemental Table 1).

Indole Acid Series. When section A is an indole it is unsubstituted and connected only to the linker, any substitutions lead to complete loss of activity for compounds in the series. Section B is usually a benzene ring with only small substituents like methyl, methoxy, chlorine, bromine, fluorine allowed. Larger hydrophobic substituents like tert-butyl, iso-propyl lead to inactive compounds. The Linker region for this compounds series is confined to 1 to 3 atoms. One atom can be a heteroatom like oxygen, linker regions larger than 3 atoms renders compounds inactive. The best active compound in this series 57578337 has benzene ring in section B methyl ortho, meta substitution and linker size of 3 atoms. A total of 33 compounds from this series were tested in dose response assays of which 11 were found to be active (Supplemental Table 2).

Salicylic Acid and Analogs Series. A series containing a salicylic acid in section A is analogous to several anti-inflammatory drugs. The salicylic acid moiety in this series of

compounds must be unsubstituted in order for compounds to show activity against GTPases. The benzene ring in section B on the other hand can be substituted with small non-polar substituents like methyl, methoxy, halogen, isopropyl. Linker length is usually 1-4 atoms where the oxygen heteroatom connected to the salicylic acid moiety can be substituted with amine, carbonyl, carboxyl groups or a carbon atom. The most potent compound in the series is 57578338 had an unsubstituted salicylic acid moiety with 2 atom linker size and an ortho bromo substitution on the benzene ring. A total of 40 compounds were tested in dose response assays of which 16 were active on multiple GTPases targets (Supplemental Table 3).

Rac1 Activation Assays

For *in vitro* Rac1 activation measurements, DMSO or an equal volume of compounds (CID: 88706, 7345532 and 2160985) in DMSO were incubated for 10 min at 30°C with 80 ng His-Rac1 protein and 125 nM GTPγS in 50 μl of 10 mM EDTA-containing buffer (NP-HPS with 1mM DTT). Further nucleotide exchange was inhibited with the addition of MgCl₂ to a final concentration of 60 mM and transferring tubes on ice. Activated Rac1 protein was isolated from solution by adding 5 μg GST-PAK-PBD and glutathione beads and rotation at 4°C for 1 h. Activated Rac1 bound to GST-PAK-PDB was resolved by SDS-PAGE (12% gels) and analyzed by immunoblot using mAb directed against Rac1. Quantification was by densitometry.

Two methods were used to assess the impact of small molecules on GTPase activity in cells based on effector binding. Commercial GLISA kit (Cytoskeleton), with PAK effector immobilized in 96-well plates were used to analyze Cdc42 (BK-127) per manufacturer's instructions. A flow-based GTPase effector binding assay was used to test the impact of small molecules on Rac1 activation.¹²

Swiss 3T3 or HeLa cells were serum starved overnight and then treated with DMSO (negative control) or small molecules for 2 h. Cells treated with 100 ng/mL EGF for 2 min served as positive controls. Four activator compounds were tested at concentrations in the range of 3 μM-100 mM. Swiss 3T3 cells were further used to monitor reversibility of Rac activation by 888706 in the presences of previously characterized Rac1 specific inhibitor 781112.⁶ Cells were serum starved overnight and treated with DMSO (1%, negative control) or 10 μM compound in DMSO for 20-30 min. As a positive control cells were treated with 10 ng/ml EGF for 2 min. Lysis and immunoprecipitation of active Rac1 with GST-PAK-PBD immobilized on GSH beads, SDS-PAGE and immunoblotting was performed as described previously.¹³

Live Cell Microscopy

Live cell microscopy of morphological changes was carried out using a rat basophil leukemia cell line (RBL-2H3). RBL-2H3 cells were grown on coverslips overnight as described,⁴ washed and overlaid with Tyrode's buffer (10 mM Hepes, pH 7.4, 130 mM NaCl, 5 mM KCl, 1.4 mM CaCl₂, 1 mM MgCl₂, 5.6 mM Glucose and 0.1% BSA). Time lapse images were taken after addition of 10 μ M 888706 or 781112 (final concentration) at intervals of 60 s for up to 115 min. In some cases, 10 μ M 888706 was added for 40 min, after which 10 μ M 781112 was added and imaging continued or vice versa. Ligand stimulated samples were treated with 1 mg/ml DNP-BSA. Imaging was performed using a Bio-Rad confocal microscope equipped with a 60x 1.4 NA oil immersion objective and Laserssharp 3000 software.

Immunofluorescence Staining and Microscopy

RBL-2H3 cells were grown on coverslips and cultured overnight in the absence or presence of 0.03-10 μ M compounds as indicated. As a positive control, cells were stimulated with 1 mg/ml DNP-BSA for 30 min as previously described.⁴ Negative controls were left untreated or treated with 1% DMSO. Cells were washed with phosphate buffered saline, fixed with 3% paraformaldehyde, permeabilized for 5 min with 0.1% Triton X-100 in Tyrode's buffer, blocked for 1 h with 1% BSA in Tyrode's buffer, and stained for 1 h with rhodamine phalloidin (Cytoskeleton Inc.) according to manufacturer's instructions. All incubations were performed at room temperature. For imaging, samples were mounted on glass slides using ProLong® Gold antifade reagent (Invitrogen). A Zeiss LSM 510 microscope, 40x objective was used to collect images.

Microscale Thermophoresis Measurements.

Wild-type His-Cdc42 (MW 22,000) was purchased as a lyophilized powder (#CD01; Cytoskeleton, Inc.). The protein was reconstituted in distilled water to 1 mg/mL, yielding a stock of ~45 μ M protein, in 2 mM Tris pH 7.6, 0.5 mM MgCl₂, 0.5% sucrose, 0.1% dextran. The Cdc42 was labeled via an amine reactive red fluorescent dye (Monolith protein labeling kit RED-NHS, Nanotemper) in HEPES buffer (30 mM HEPES, pH 7.5, 20 mM NaCl, 100 mM KCl, 5 mM EDTA) according to manufacturer's instructions and designed to yield labeling efficiency of ~1 fluorophore/protein. The final protein concentration was measured after removal of excess dye and diluted to 20 μ M in Thermophoresis Buffer (HEPES buffer containing 1 mM DTT, 1

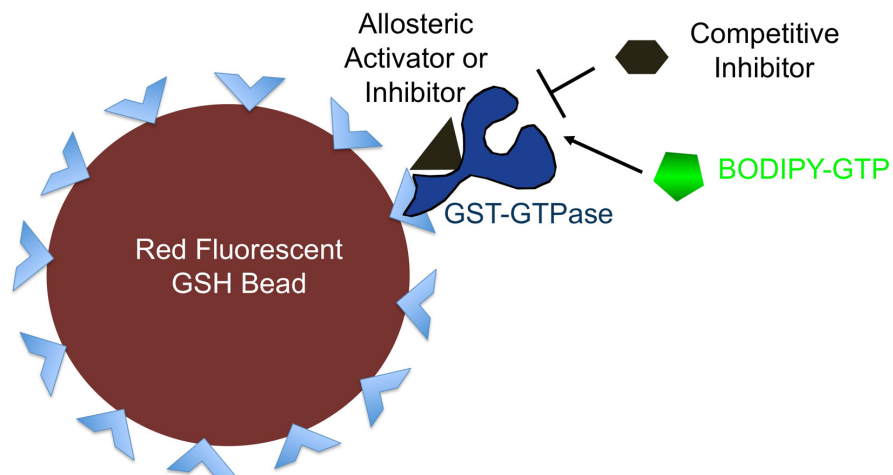
mg/ml BSA, 0.05% NP-40). Activator 888706 stock (30 mM in DMSO) was diluted to 30 or 50 μ M in Thermophoresis buffer and further serially diluted (1.53 nM to 25 μ M compound) for Cdc42 binding measurements. Red fluorescently labeled Cdc42 was added to 200 nM final immediately prior to loading of each activator dilution into microscale thermophoresis S-capillaries. Measurements were conducted on a Monolith NT.115 at 24°C, using 70% excitation power, and 40% MST power for up to 30 s. The response amplitude ranged from 1.6-2.04 in two independent trials.

Statistical Analyses

Prism 5 software (GraphPad) was used to analyze quantitative biochemical, flow cytometry and GLISA data to determine statistical significance. One-way ANOVA (Analysis of Variance) with Dunnett's test for multiple comparisons was performed to compare differences between the means of each group relative to the control group for all assays. P-values less than 0.05 were considered statistically significant. A MatLab algorithm was used to quantify cell shape changes (Figure S5).

Supplementary Figures

a. HTS Assay for Small Molecule Activators or Inhibitors of GTP-binding



b. Multiplex HTS using Graded Intensity Red Fluorescent Beads bearing Individual GTPases (Rab, Ras and Rho-family) and BODIPY-GTP

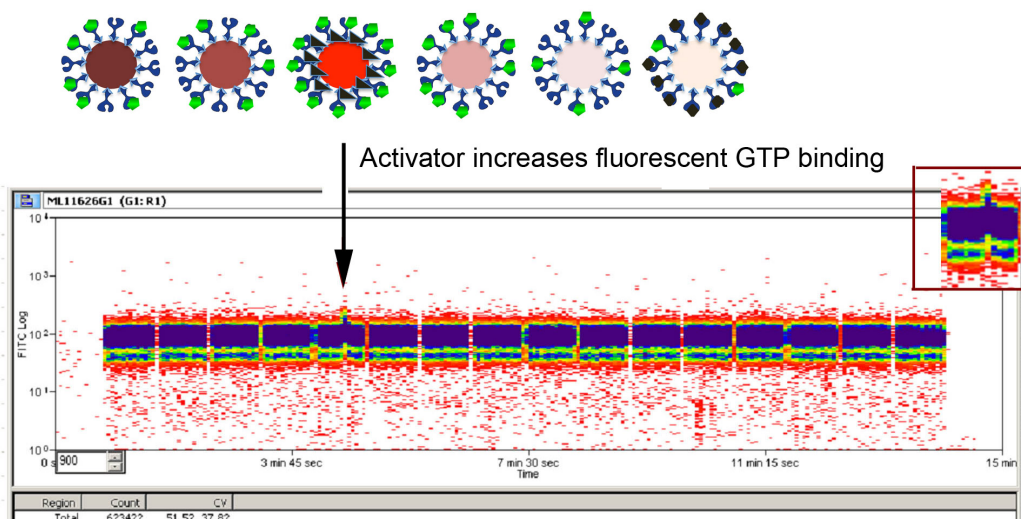


Figure S1. High throughput screen identifies small molecule activators of Ras GTPase superfamily. (a) Schematic of HTS assay measuring fluorescent BODIPY-GTP binding to GST-GTPases immobilized on GSH beads suited for flow cytometry. (b) For multiplex HTS primary screen GST-GTPases (five different wild-type GTPases and three constitutively activated mutants (Cdc42, activated Cdc42Q61L, Rab2, Rab7, Rac1, activated Rac1Q61L, H-Ras, activated H-RasG12V) were conjugated to fluorescent GSH-beads of varying red fluorescence intensity. Assays were conducted in the presence of EDTA, initiated with the addition of BODIPY-GTP and library compounds in 384 well plates. HyperCyt time-resolved data (time versus logarithm of green fluorescence) collected in the FL8 red fluorescence channel are shown for one 384-well plate. Each block represents a group of 20 samples, separated by blank wells. Each sample contains data for 6 targets as indicated in the text and a GST-GFP control (Y axis:

fluorescence intensity, X axis: time). Arrow denotes positive well with increased fluorescent nucleotide binding. The well contained SID57578335 (CID888706), inset 2x magnification of GTPase activator seen as increased fluorescence in primary screen, $n=1$. Inhibitors were identified in same screen as compounds that decreased fluorescence (illustrated by bead on the far right). A total of 194,635 compounds were screened of which 1877 were identified as actives representing 738 unique compounds. Z' values were Rac1 and Rab7 0.85 ± 0.04 , Rab2 0.86 ± 0.04 , Cdc42 0.87 ± 0.04 , HRas and activated Rac1Q61L mutant, 0.9 ± 0.03 (Panel b previously shown in as part of Fig. 1 in probe report).

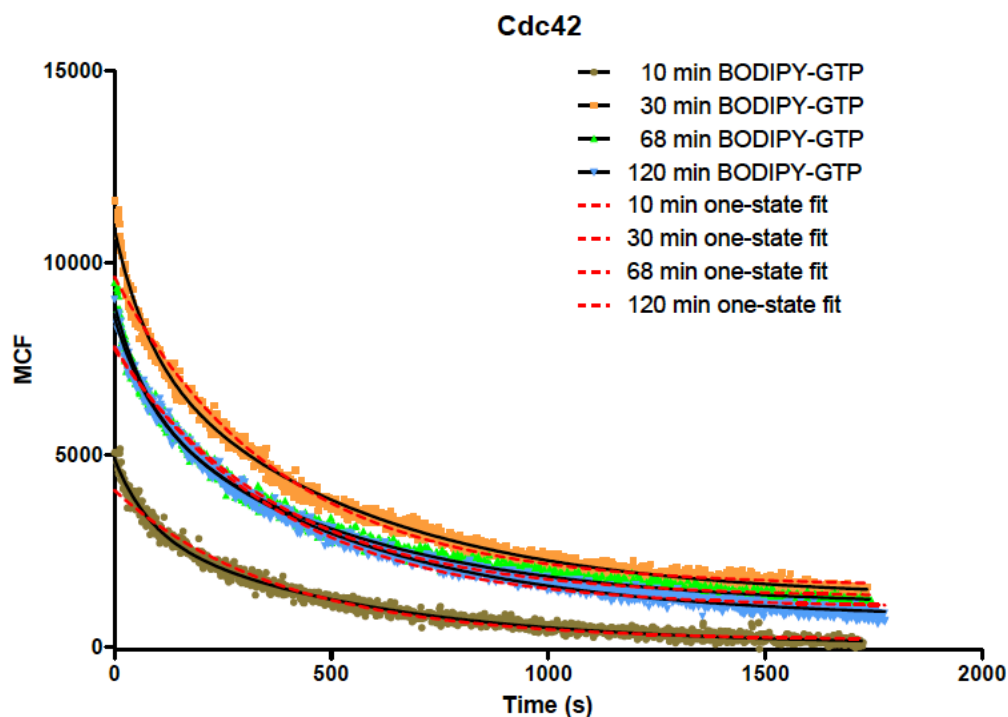


Figure S2. The nucleotide exchange from Cdc42-conjugated beads in the presence of small molecule activator fits to a two-phase exponential equation. BODIPY-GTP dissociation rate from Cdc42-conjugated beads was measured after pre-incubation with 10 μ M activator 888706 and BODIPY-GTP association for 10-120 min. are plotted as MCF versus time after the addition of 200 μ M GTP. Data from Figure 3e fitted with one-phase exponential fit (dotted red lines) and two-phase exponential fit (solid black lines). NB: A biphasic dissociation rate is expected to give rise to an apparent K_d that reflects the heterogeneity arising from and weighted by the two dissociation rates. The half-time for interconversion between states is estimated to be ~ 5 h. Thus, even at high activator concentration (10 μ M), the K_d is not expected to vary in proportion to the ratio of the two dissociation rates when the interconversion between the two states is incomplete.

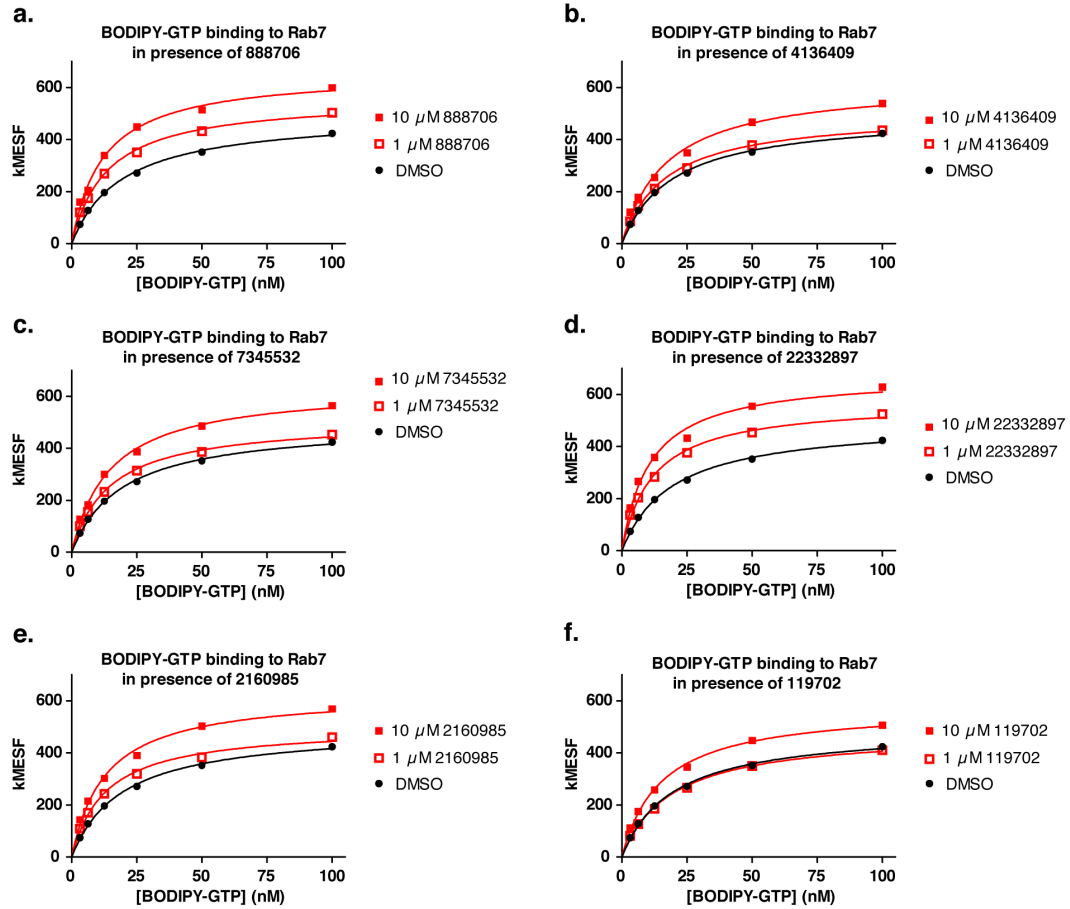


Figure S3. . Representative effect of activators on equilibrium binding of BODIPY-GTP to Rab7. Rab7-conjugated beads were incubated with increasing concentrations of BODIPY-GTP in the presence of either 1% DMSO, 1 μ M activator, or 10 μ M activator. Each set of binding curves were fitted to a hyperbola by least squares fit via GraphPad Prism, resulting in Apparent B_{\max} and Apparent K_d .

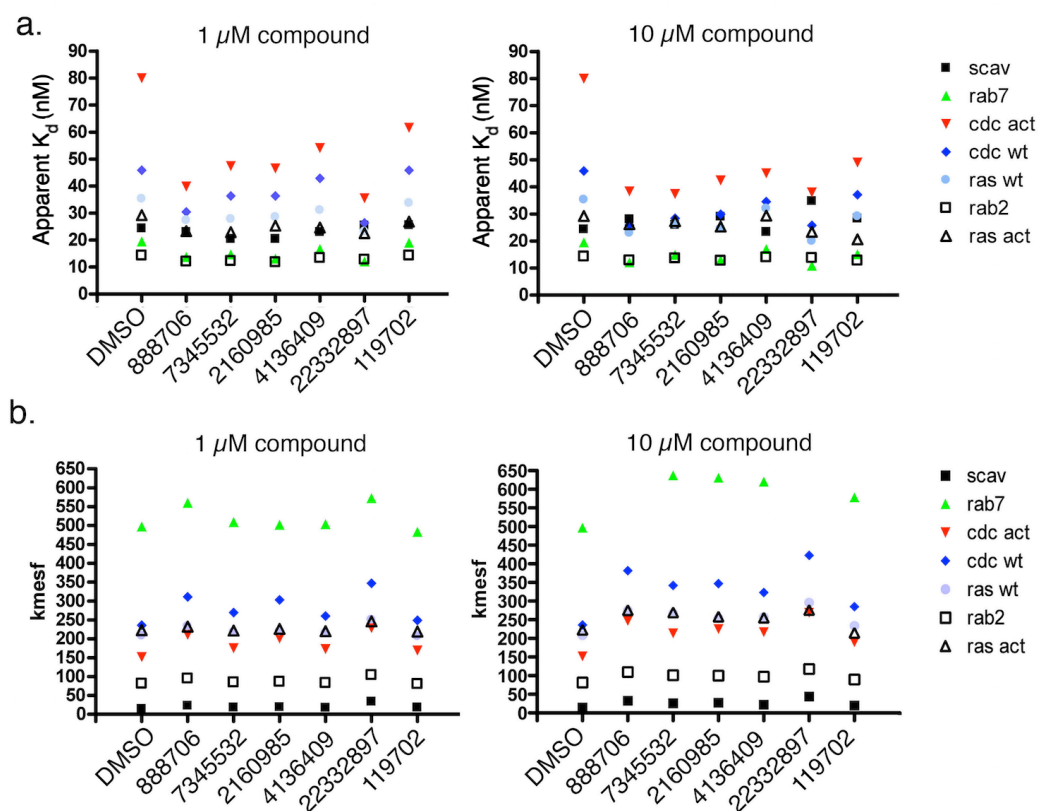
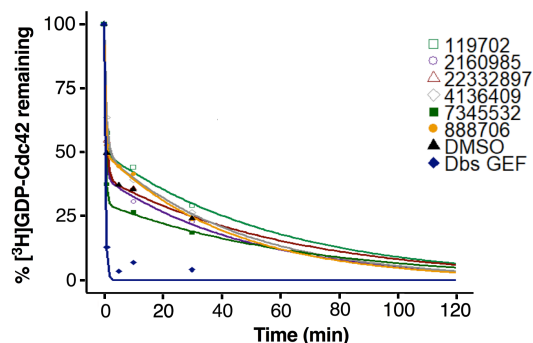


Figure S4. Small molecule activators increase nucleotide binding affinity by decreasing Apparent K_d . Simultaneous measurements of the steady state GTP-binding of six GTPases and one control (scavenger, scav) were performed as a function of the concentration of fluorescent GTP (0-100 nM) in the presence of DMSO, or an activator compound (1 or 10 μ M). Plotted are (a) Apparent K_d , nM and (b) Apparent B_{max} , kilo molecules of equivalent soluble fluorochrome (kMESF) values on six GTPase targets and scavenger control beads; $n=2$.



Condition	Time till 5% baseline (min)
119702	137
2160985	105
22332897	133
4136409	107
7345532	121
888706	100
DMSO	19
Dbs GEF	1.5

Figure S5. A single-phase exponential decay model was used to fit the nucleotide exchange data in the presence of the Dbs GEF. A two-phase exponential decay model (statistical software R version 3.4.4) was used to fit the data as a combination of a fast and slow exponential decay for the compounds. The equation used is: $Y = S_1 * e^{-K_1 t} + S_2 * e^{-K_2 t}$, where $S_1 + S_2 = 100$. The Gauss-Newton algorithm was used to estimate the parameters by minimizing the sum of squares of errors between the data and model predictions. Predicted time to approach the baseline (5% [3 H]GDP remaining) for each of the compound and controls is shown in the table.

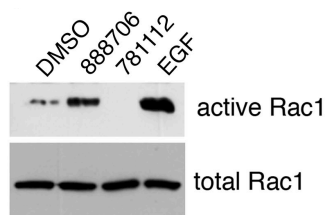


Figure S6. Swiss 3T3 cells were serum starved overnight, treated with DMSO (control, 10 μ M CID888706 (activator), 10 μ M CID781112 (inhibitor) or with growth factor (EGF). Top blot shows active Rac isolated on GST-PAK-PBD beads and bottom blot shows total Rac in each lysate as a protein loading control, n=2 (Subset of data previously shown in Fig. 3 of Probe report).

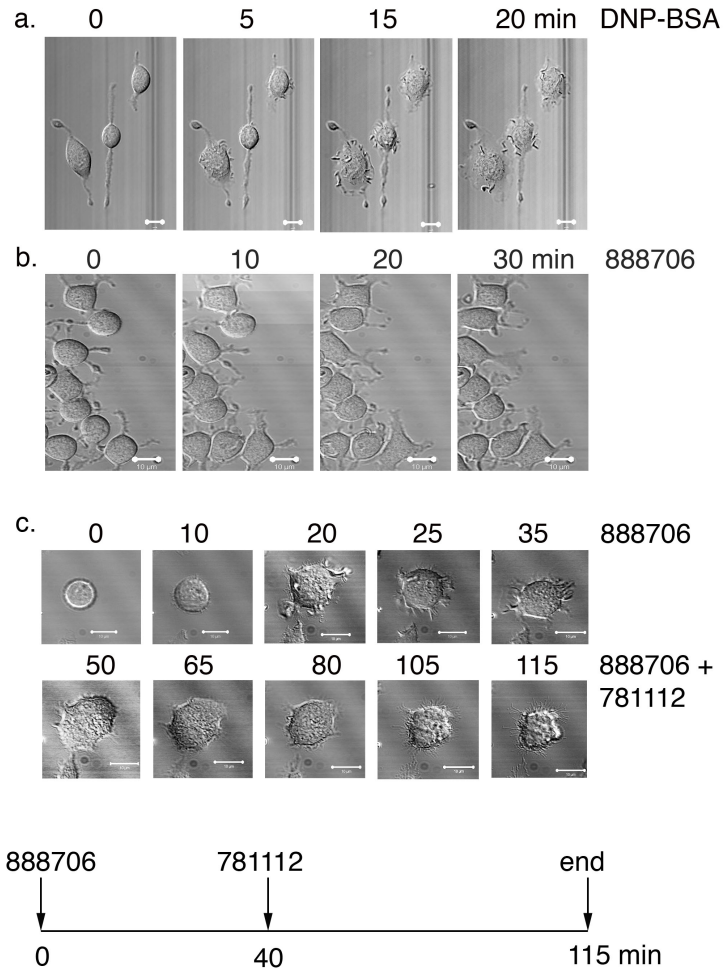


Figure S7. Live cell microscopy demonstrates rapid and reversible cell response to addition of small molecule activator. Live RBL-2H3 cells were monitored by DIC microscopy on a Zeiss inverted microscope for up to 115 min. Bars 10 μm . (a) Resting RBL-2H3 cells with DMSO ($t=0$) were stimulated with DNP-BSA (5-20 min), $n=3$. (b) RBL-2H3 cells incubated with 10 μM 888706 (0-30 min), $n=3$ (Panel b previously shown as part of Fig. 5 of probe report). (c) RBL-2H3 cells treated with 10 μM 888706 (activator) for 40 min, after which 10 μM 781112 (irreversible inhibitor) was added for remaining time course (41-115 min), $n=2$. Schematic shows experimental flow chart.

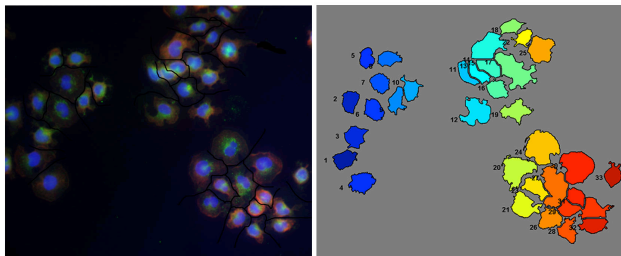


Figure S8. Matlab was used to devise an algorithm for automatically detecting cell edges and quantifying cell areas. Top panel shows immunostained cells: red-actin stained with rhodamine phalloidin, blue-nuclei stained with DAPI, green-PAK stained specific antibody and FITC-conjugated secondary. Image taken on Zeiss Axioskop with AxioCam color camera. Bottom panel shows outlined cells and area calculation.

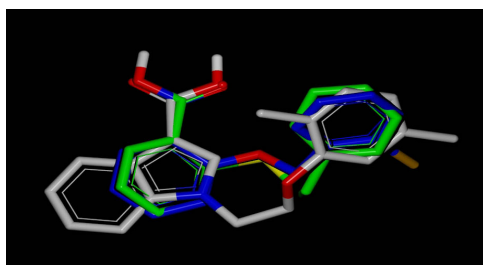


Figure S9. ROCS shape overlay for the compounds: 888706 is depicted in green, 345532 is depicted in gray, and 2160985 is depicted in blue.

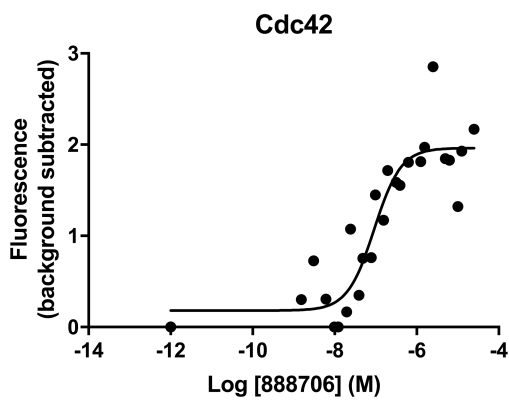
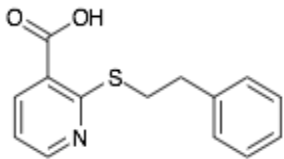
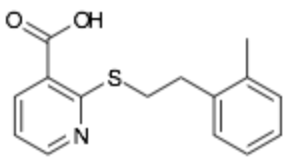
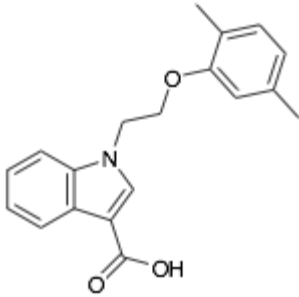
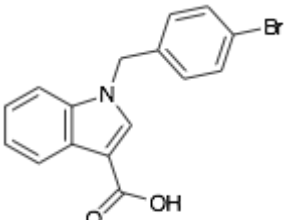
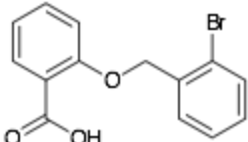
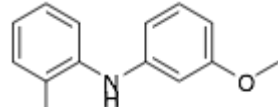


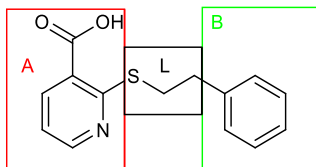
Figure S10. Equilibrium binding of activator 888706 to Cdc42 wt measured via microscale thermophoresis is graphed as fluorescence after background subtraction versus concentration of 888706, including sigmoidal curve fit by GraphPad Prism resulting in EC50 of 90 nM (n=2). A few data points at extremely low and high concentrations were excluded.

Table S1. Summary of Lead Activators. Apparent K_d and apparent B_{max} values based on equilibrium binding across varying BODIPY-GTP (2.5-100 nM) concentrations in the presence of 1% DMSO (control) or 10 μ M activator.

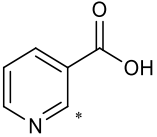
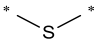
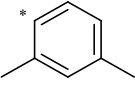
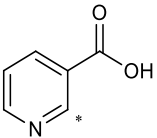
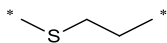
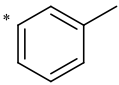
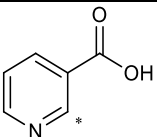
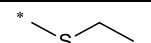
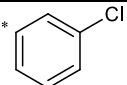
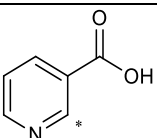
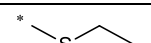
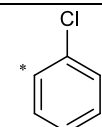
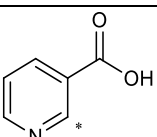
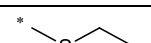
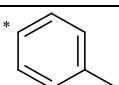
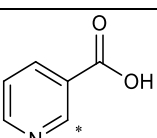
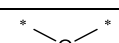
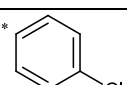
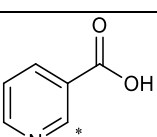
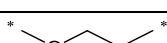
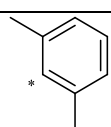
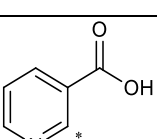
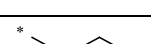
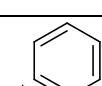
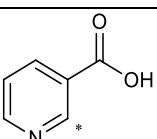
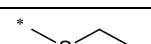
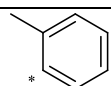
 <p>CID 888706</p>	 <p>CID 4136409</p>	 <p>CID 7345532</p>
2-phenethylsulfanylpuridine-3-carboxylic acid	2-[(3-methylphenyl)methylsulfanyl]pyridine-3-carboxylic acid	1-[2-(2,5-dimethylphenoxy)ethyl]indole-3-carboxylic acid
 <p>CID 22332897</p>	 <p>CID 2160985</p>	 <p>CID 119702</p>
1-[(4-bromophenyl)methyl]indole-3-carboxylic acid	2-[(2-bromophenyl)methoxy]benzoic acid	2-[(3-methoxyphenyl)amino]benzoic acid

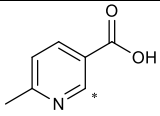
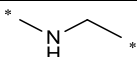
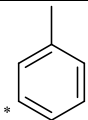
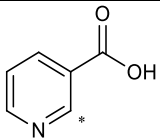
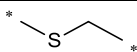
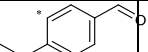
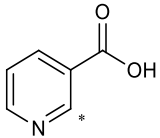
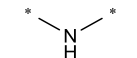
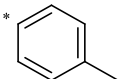
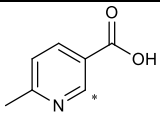
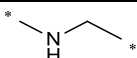
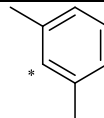
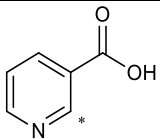
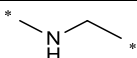
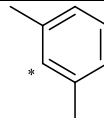
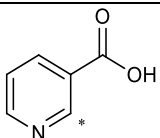
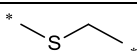
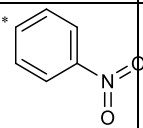
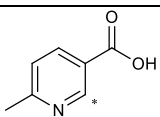
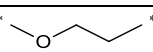
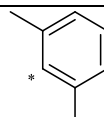
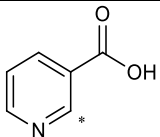
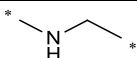
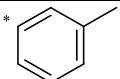
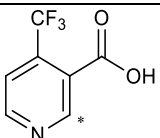
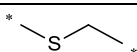
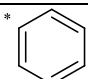
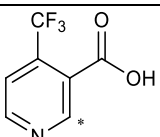
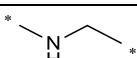
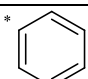
CID	Log P	Log S	Apparent K_d nM							Apparent B_{max} kMESF						
			Cdc 42 Act	Cdc 42 WT	Rab 2 WT	Rab 7 WT	H-Ras Act	H-Ras WT	Scav	Cdc 42 Act	Cdc 42 WT	Rab 2WT	Rab 7 WT	H-Ras Act	H-Ras WT	Scav
DMSO	-	-	80.0 0	45.8 5	14.3 0	19.4 3	29.2 0	35.3 0	24.3 5	152. 00	236. 00	81.2 5	497. 00	222. 70	208. 00	14.2 3
888706	3.34	-3.76	38.3 7	25.9 0	12.8 3	12.1 0	26.2 2	23.0 0	28.0 0	247. 40	381. 60	109. 90	658. 50	275. 20	274. 70	33.0 0
4136409	3.31	-3.72	45.0 0	34.5 7	14.0 0	17.0 0	29.4 0	32.0 0	23.3 6	217. 00	323. 00	97.0 0	620. 60	255. 60	257. 00	22.0 0
7345532	5.28	-4.7	37.4 0	28.4 0	13.6 0	14.8 5	27.3 5	26.2 1	26.0 0	213. 90	342. 00	100. 80	637. 40	269. 40	266. 70	25.5 6
22332897	4.89	-4.43	38.0 0	25.8 0	13.7 6	10.8 7	23.3 6	20.0 0	34.7 7	269. 00	423. 00	118. 00	675. 00	276. 00	296. 00	44.0 0
2160985	4.22	-4.56	42.4 0	29.8 5	12.6 9	13.0 0	25.2 8	24.5 8	29.0 0	225. 00	347. 00	100. 00	630. 70	258. 00	254. 50	27.2 3
119702	4.32	-3.78	48.9 8	37.1 0	12.8 1	15.1 5	20.5 7	29.1 6	28.3 3	190. 00	285. 00	89.7 0	578. 00	215. 00	233. 70	19.6 0

Table S2. Nicotinic Acid SAR Series and Dose Response Data for In Vitro Activation of Fluorescent GTP-Binding.



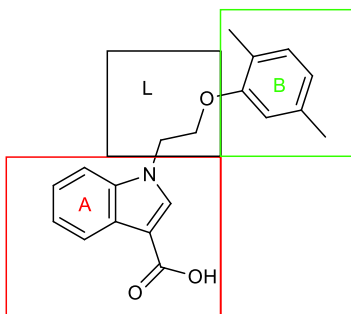
PUB CHE M CID	A	L	B	Log EC ₅₀ Cdc4 2Act	Log EC ₅₀ Cdc4 2WT	Log EC ₅₀ Rab2 WT	Log EC ₅₀ Rab7 WT	Log EC ₅₀ Rac1 Act	Log EC ₅₀ Rac1 WT	Log EC ₅₀ Ras Act	Log EC ₅₀ Ras WT
8887 06				7.23	7.00	6.45	6.74	7.59	7.70	7.02	6.85
2510 9948				5.79	5.66	5.65	5.76	6.12	5.66	5.75	5.61
2510 9947				5.51	5.30	6.23	5.87	5.88	5.72	5.45	
4136 409				6.72	6.52	7.13	6.97	6.76	7.14		6.37
4095 681				6.44	6.39	6.68	6.54	6.77	7.29		6.13
7626 62				5.38	5.29	5.49	5.62	5.33	5.04		5.30
4249 711				6.62	6.63	6.58	6.88	6.79	6.15		

2560 348				5.50	5.48	5.17	5.97	5.95		5.96	5.73
2510 9949				5.94	5.72	5.85	6.00	6.14	5.80	5.63	5.64
4136 404				6.06	5.86	5.89		5.82	5.71		5.76
7574 12				5.91	5.75	5.61		5.85	5.41		5.62
7577 77				5.95	6.07		6.33	5.98	5.70	6.07	5.96
6094 54				5.27	5.17		5.39	5.41	5.00		
2510 9945				5.54	5.08			5.78	5.39	5.82	
7577 79				4.85			5.31	5.74	5.51	5.70	5.64
3336 645				6.10	6.03	5.99	6.27	6.22	5.92		6.18

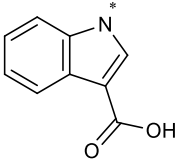
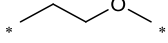
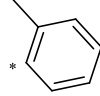
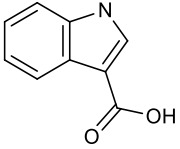
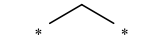
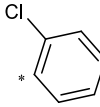
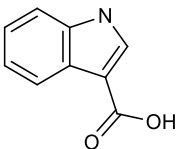
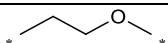
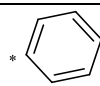
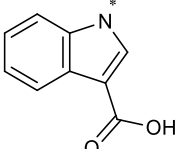
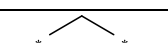
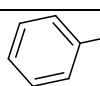
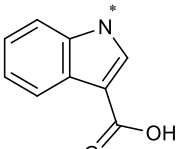
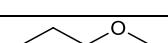
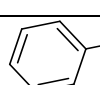
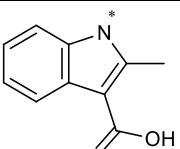
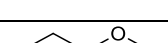
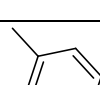
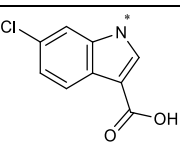
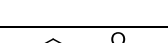
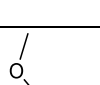
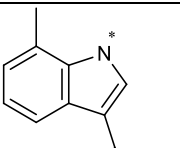
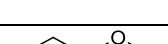
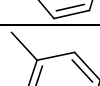
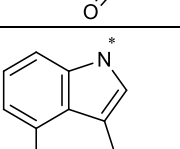

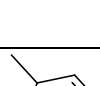
2510 9943											
3474 318											
5298 375											
2510 9940											
2510 9939											
6732 35											
2510 9946											
2510 9942											
2510 9950											
2510 9938											

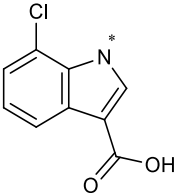
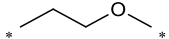
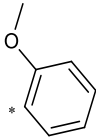
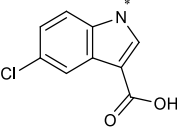
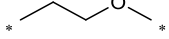
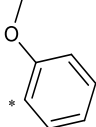
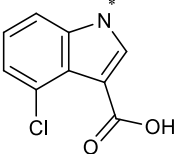
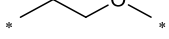
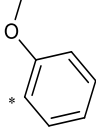
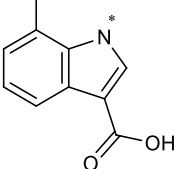
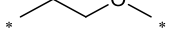
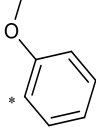
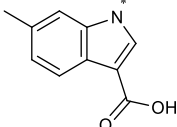
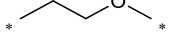
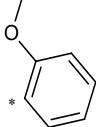
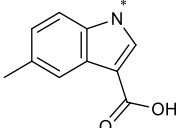
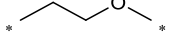
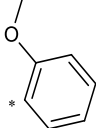
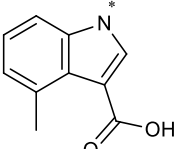
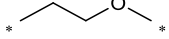
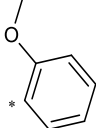
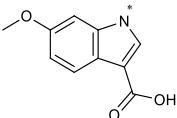
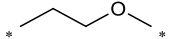
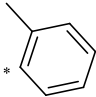
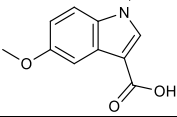
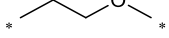
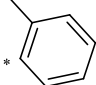
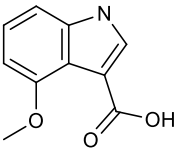

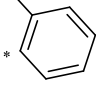
*Compounds identified by virtual screening and purchased from ChemDiv. Actives in secondary screens are in bold and include dose response data, all others were inactive.

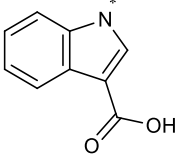

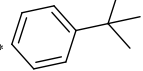
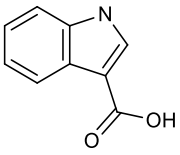
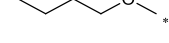
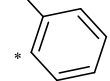
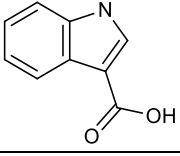
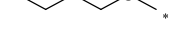
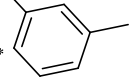
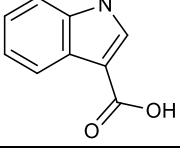

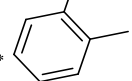
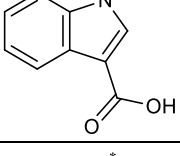


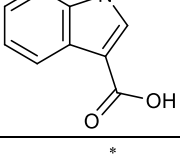

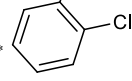
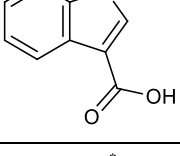

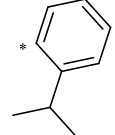
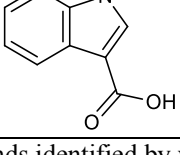

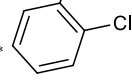
Table S3. Indole SAR Series and Dose Response Data for In Vitro Activation of Fluorescent GTP-Binding.



Pubchem CID	A	L	B	Log EC ₅₀ Cdc42 Act	Log EC ₅₀ Cdc4 2WT	Log EC ₅₀ Rab2 WT	Log EC ₅₀ Rab7 WT	Log EC ₅₀ Rac1 Act	Log EC ₅₀ Rac1 WT	Log EC ₅₀ Ras Act	Log EC ₅₀ Ras WT
3161159				6.13	5.87	6.30	6.46	6.22	5.89	6.33	6.09
2986991				5.90	5.84	6.11	6.29	6.36	5.88		5.96
7345532				6.45	6.23	6.80	7.11	6.65	6.10	6.71	6.46
22332897				6.78	6.53	6.84		7.16	6.91		6.83
16194519				5.56	5.52			5.26	5.09	6.60	5.57
3161160				4.32		5.15		5.06			4.55

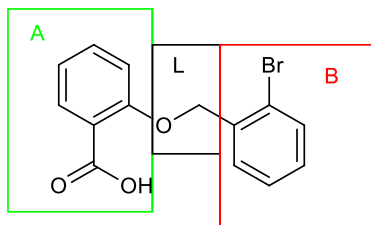
161955 85						5.48		6.29	5.77		
155882 46				6.24							
298833 5								6.07	5.26		
374427 0									7.35		
161945 18								5.94			
251099 74											
251099 72											
251099 76											
251099 75											

251099 73											
251099 71											
251099 70											
251099 69											
251099 68											
251099 67											
251099 66											
251099 65											
251099 64											
251099 63											

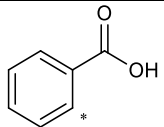
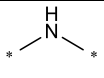
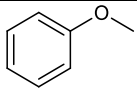
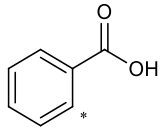
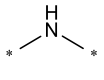
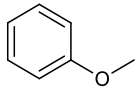
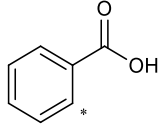
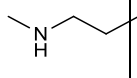
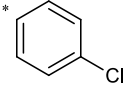
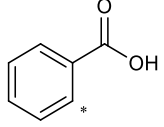
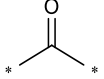
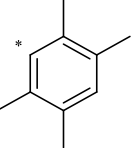
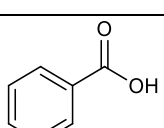
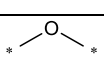
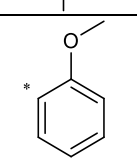
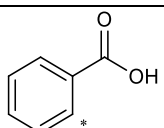
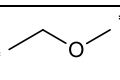
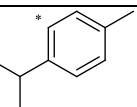
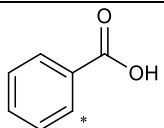
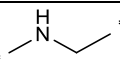
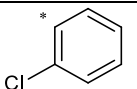
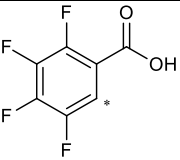
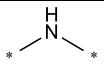
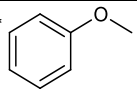
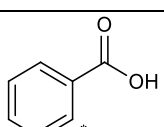
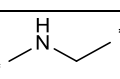
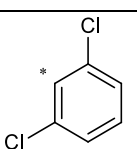
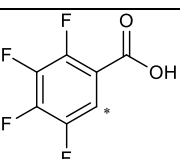
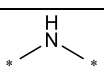
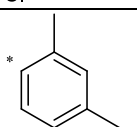
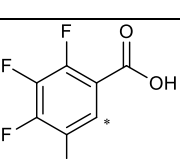
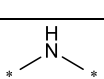
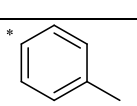
251099 16											
223329 02											
223329 03											
223328 98											
223328 99											
223329 04											
223329 01											
223329 00											

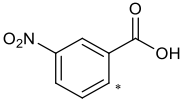
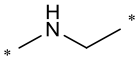
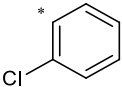
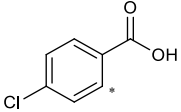
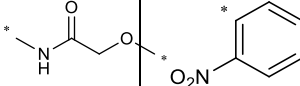
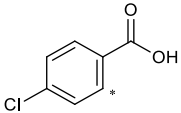
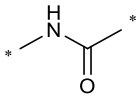
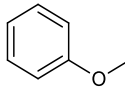
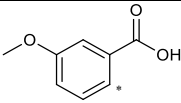
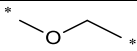
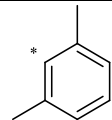
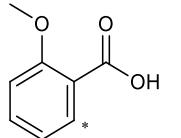
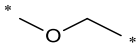
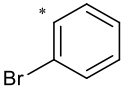
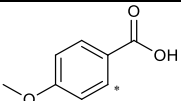
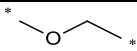
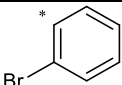
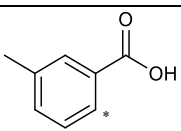
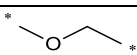
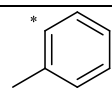
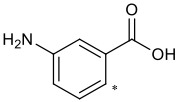
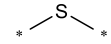
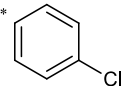
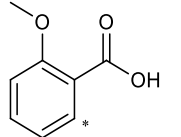
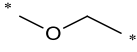
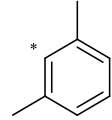
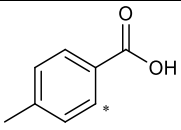
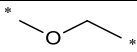
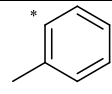
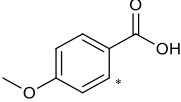
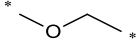
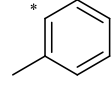
*Compounds identified by virtual screening and purchased from ChemDiv. Actives in secondary screens are in bold and include dose response data, all others were inactive.

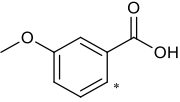
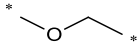
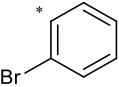
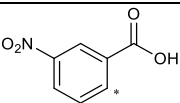
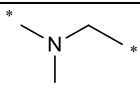
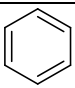
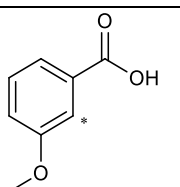
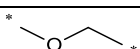
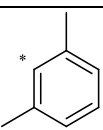
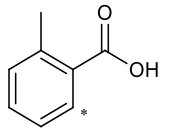
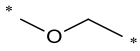
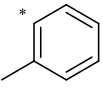
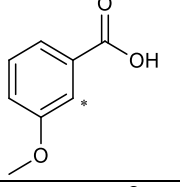
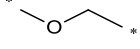
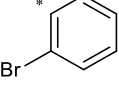
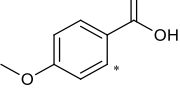
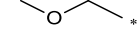
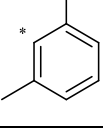
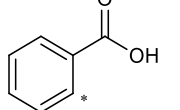
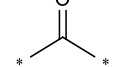
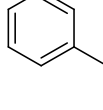
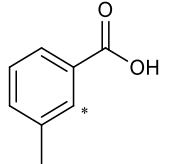
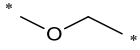
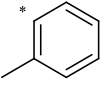
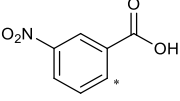
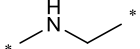
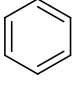
Table S4. Salicylic Acid and Analogs SAR Series and Dose Response Data for In Vitro Activation of Fluorescent GTP-Binding.



PUBCH EM CID	A	L	B	Log EC ₅₀ Cdc4 2 Act	Log EC ₅₀ Cdc4 2 WT	Log EC ₅₀ Rab2 WT	Log EC ₅₀ Rab7 WT	Log EC ₅₀ Rac1 Act	Log EC ₅₀ Rac1 WT	Log EC ₅₀ Ras Act	Log EC ₅₀ Ras WT
216098 5				7.30	6.99	6.60	7.69	7.09	6.82	7.03	6.96
773648				6.39	6.18	6.90	7.05	6.75	6.34		6.41
31736				6.26	6.23	6.18	6.59	5.90	5.86	5.86	5.89
236090 2				6.17	5.97	6.14	6.01	6.41	6.73	6.09	5.99
231260 1				4.86	4.87	4.46	4.63	5.37	5.77	4.84	4.90
75237				5.65	5.47	5.55	5.46	5.11	4.84	5.47	
708212				5.97	5.79	5.94	6.07	5.97	5.40		5.78
353852 2				6.25	6.30	6.75	7.36		5.84		
304868				5.32	4.97	4.93		5.76	5.21		4.91

119702				6.56	6.44	6.55		6.95	6.34		6.46
202918				5.55	5.58	5.97		5.86			
772133 7				6.05	5.81		6.47		5.82		
803711				5.31	5.23				5.21		
578689				5.05			5.57	5.08	4.80	5.20	4.95
150855 5				5.99			6.50		5.81		
773657									6.05		
139957 6											
498756 4											
454915 4											
454914 6											

3713420											
976704											
1254149											
25109960											
25109951											
25109953											
25109956											
5298562											
25109959											
25109957											
20988506											

251099 52											
461229 2											
251099 62											
251099 55											
251099 54											
251099 61											
66563											
251099 58											
294233 7											

*Compounds identified by virtual screening and purchased from ChemDiv. Actives in secondary screens are in bold and include dose response data, all others were inactive.

References

- [1] McEwen, D. P., Gee, K. R., Kang, H. C., and Neubig, R. R. (2001) Fluorescent BODIPY-GTP analogs: Real-time measurement of nucleotide binding to G proteins, *Anal Biochem* 291, 109-117.

- [2] Schwartz, S. L., Tessema, M., Buranda, T., Pylypenko, O., Rak, A., Simons, P. C., Surviladze, Z., Sklar, L. A., and Wandering-Ness, A. (2008) Flow cytometry for real-time measurement of guanine nucleotide binding and exchange by Ras-like GTPases, *Anal Biochem* 381, 258-266.
- [3] Simons, P. C., Young, S. M., Carter, M. B., Waller, A., Zhai, D., Reed, J. C., Edwards, B. S., and Sklar, L. A. (2011) Simultaneous in vitro molecular screening of protein-peptide interactions by flow cytometry, using six Bcl-2 family proteins as examples, *Nat Protoc* 6, 943-952.
- [4] Wilson, B. S., Kapp, N., Lee, R. J., Pfeiffer, J. R., Martinez, A. M., Platt, Y., Letourneur, F., and Oliver, J. M. (1995) Distinct functions of the Fc epsilon R1 gamma and beta subunits in the control of Fc epsilon R1-mediated tyrosine kinase activation and signaling responses in RBL-2H3 mast cells, *J Biol Chem* 270, 4013-4022.
- [5] Green, H., and Meuth, M. (1974) An established pre-adipose cell line and its differentiation in culture, *Cell* 3, 127-133.
- [6] Surviladze, Z., Waller, A., Wu, Y., Romero, E., Edwards, B. S., Wandering-Ness, A., and Sklar, L. A. (2010) Identification of a Small GTPase Inhibitor Using a High-Throughput Flow Cytometry Bead-Based Multiplex Assay, *J Biomol Screen* 15, 10-20.
- [7] Kuckuck, F. W., Edwards, B. S., and Sklar, L. A. (2001) High throughput flow cytometry, *Cytometry* 44, 83-90.
- [8] Zhang, J. H., Chung, T. D., and Oldenburg, K. R. (1999) A Simple Statistical Parameter for Use in Evaluation and Validation of High Throughput Screening Assays, *J Biomol Screen* 4, 67-73.
- [9] Rush, T. S., Grant, J. A., Mosyak, L., and Nicholls, A. (2005) A shape-based 3-D scaffold hopping method and its application to a bacterial protein-protein interaction, *J Med Chem* 48, 1489-1495.
- [10] Grant, J. A., Gallardo, M. A., and Pickup, B. T. (1996) A fast method of molecular shape comparison: A simple application of a Gaussian description of molecular shape, *J Comput Chem* 17, 1653-1666.
- [11] Tessema, M., Simons, P. C., Cimino, D. F., Sanchez, L., Waller, A., Posner, R. G., Wandering-Ness, A., Prossnitz, E. R., and Sklar, L. A. (2006) Glutathione-S-transferase-green fluorescent protein fusion protein reveals slow dissociation from high site density beads and measures free GSH, *Cytometry A* 69, 326-334.
- [12] Buranda, T., BasuRay, S., Swanson, S., Agola, J., Bondu, V., and Wandering-Ness, A. (2013) Rapid parallel flow cytometry assays of active GTPases using effector beads, *Anal Biochem* 442, 149-157.
- [13] Benard, V., and Bokoch, G. M. (2002) Assay of Cdc42, Rac, and Rho GTPase activation by affinity methods, *Methods Enzymol* 345, 349-359.
- [14] Surviladze, Z., Ursu, O., Miscioscia, F., Curpan, R., Halip, L., Bologa, C., Oprea, T., Waller, A., Strouse, J., Salas, V., Wu, Y., Edwards, B., Wandering-Ness, A., and Sklar, L. (2010) Three small molecule pan activator families of Ras-related GTPases, In *Probe Reports from the NIH Molecular Libraries Program*, Bethesda (MD).